

## Crystal structure of hillebrandite: A natural analogue of calcium silicate hydrate (CSH) phases in Portland cement

YONGSHAN DAI

Garber Research Center, Harbison-Walker Refractories, 1001 Pittsburgh-McKeesport Boulevard, West Mifflin, Pennsylvania 15122, U.S.A.

JEFFREY E. POST

Department of Mineral Sciences, Smithsonian Institution, Washington, DC 20560, U.S.A.

### ABSTRACT

The crystal structure of hillebrandite,  $\text{Ca}_2\text{SiO}_3(\text{OH})_2$ , was solved and refined in space group  $Cmc2_1$ ,  $a = 3.6389$ ,  $b = 16.311$ ,  $c = 11.829$  Å, to  $R = 0.041$  using single-crystal X-ray data. The structure consists of a three-dimensional network of Ca-O polyhedra that accommodates wollastonite-type Si-O tetrahedral chains. Each of the wollastonite-type chains is an average of two symmetrically equivalent chains related by the mirror plane perpendicular to **a**. In a given structural channel of the Ca-O polyhedral network, only one chain orientation can be occupied to give reasonable Si-O distances. The O3 and O4 sites corresponding to each vacant Si2 site are occupied by OH groups to achieve charge balance. The wollastonite-type Si-O tetrahedral chains in the hillebrandite structure resemble those reported for many calcium silicate hydrate (CSH) phases.

### INTRODUCTION

Hillebrandite,  $\text{Ca}_2\text{SiO}_3(\text{OH})_2$ , is one natural member of the  $\text{CaO-SiO}_2\text{-H}_2\text{O}$  ternary system, which includes numerous natural and synthetic calcium silicate hydrate (CSH) phases, most with a common unit-cell axis of about 3.64 or  $2 \times 3.64$  Å and a fibrous crystal habit along this axis. Many of these compounds are the major hydration products of Portland cement and the main strength-forming phases in steam-cured mortar cement. Despite the great interest in the atomic arrangements of the CSH phases by cement chemists as a key to understanding the hydration mechanism and strength development of Portland cement paste, understanding of the CSH structures is far from satisfactory, even after decades of intensive research. To date, no material suitable for single-crystal X-ray study has been synthesized. Natural minerals that are analogous to the CSH phases have been subjected to numerous crystallographic investigations. Unfortunately, significant progress in those studies also has been limited by lack of crystals suitable for single-crystal diffraction studies. Powder X-ray diffraction studies (Heller, 1953) have shown that hillebrandite resembles a synthetic  $\beta\text{-Ca}_2\text{SiO}_4 \cdot \text{H}_2\text{O}$  phase and the CSH(II) cement phases described by Taylor (1986), Gard and Taylor (1976), and others, which are the main components in concrete and lime-silica products formed during the binding process. As part of a larger study of cement-related minerals, we present here the details of the crystal structure of hille-

brandite and comment upon the structural relationships of hillebrandite with other CSH phases.

### EXPERIMENTAL METHODS

After an exhaustive examination of many hillebrandite samples, a fragment of a specimen (NMNH 95767-7) from Velardena, Durango, Mexico, was found to be suitable for structure determination. Microscope examination under polarized light and systematic precession photographic studies revealed that the selected crystal fragment contained about 10% misaligned hillebrandite fibers, but it was the best crystal found from the samples. The overexposed precession films taken along **a**, **b**, and **c** axes did not show any evidence of the superstructure reflections suggested by earlier investigators (Heller, 1953; Ishida et al., 1992). The systematic absences on the films suggested possible space groups  $Cmc2_1$ ,  $Cmcm$ , and  $Ama2$ .

Intensity data were collected on an Enraf Nonius CAD4 diffractometer utilizing graphite-monochromated  $\text{MoK}\alpha$  radiation for the diffraction sphere. Unit-cell parameters (Table 1) were refined using diffraction angles from 25 automatically centered reflections ( $2\theta = 20\text{--}36^\circ$ ). Other details of data measurement are presented in Table 1. Examination of the intensity and orientation standards showed no significant deviations. The intensity data were corrected for Lorentz and polarization effects, and absorption effects were corrected utilizing  $\pm 180^\circ$   $\phi$ -scans at  $10^\circ$  intervals for six reflections. After converting the in-

TABLE 1. Crystal and experimental data

Crystal size (mm)	0.040 × 0.060 × 0.150
Space group	<i>Ccm2</i> <sub>1</sub> (no. 36)
Z	6
Cell parameters	
<i>a</i> (Å)	3.6389(8)
<i>b</i> (Å)	16.311(5)
<i>c</i> (Å)	11.829(3)
<i>V</i> (Å <sup>3</sup> )	702.1(3)
$\theta$ limit (°)	1–30
Reciprocal space	$\pm h, \pm k, \pm l$
Standards	
Orientation	3 per 400 refls.
Intensity	3 per 5 h
Total data collected	6807
Unique data	1056
$F > 2\sigma_F$ data	325
$R_{\text{merge}}$ (% on $F_{\text{obs}}$ )	6.5
$R$ (%)	4.1
$R_w$ (%)	4.5
Goodness-of-fit	0.86
Final difference maps (e/Å <sup>3</sup> )	
(+)	0.69
(-)	1.05

tensity data to structure factors, symmetry-equivalent reflections were averaged. In the final cycle of full-matrix least-squares refinement, only the reflections with  $F > 2\sigma_F$  were used, and the observed reflections were weighted proportionally to  $\sigma_F^{-2}$ , with a term to reduce the weighting of intense reflections (Fair, 1990).

Crystallographic calculations were made using the programs of the Molen (Fair, 1990) package on a VAX3100 workstation. The E statistics strongly indicated the absence of a center of symmetry, and subsequent structure determination revealed that *Ccm2*<sub>1</sub> (no. 36) is the correct space group. Direct methods were used for phase determination. The subsequent electron density map revealed three Ca, one Si (Si1), and several O positions. These positions are all located on the  $4a$  (0,*y*,*z*) special position on the mirror planes (Table 2). Fourier difference map calculations located the O7, O8, and half-occupied Si2 sites. The refinement, then, converged to  $R \approx 0.045$  with all cations anisotropic and all anions isotropic. The unusual anisotropic displacement factors of the Si1 site and abnormal Si1-O distances suggest splitting of the site and displacement from the mirror plane onto the  $8b$  (*x*,*y*,*z*) general position. The two disordered Si1 sites, related by the mirror, are about 0.5 Å apart. The final full-matrix

TABLE 2. Atomic parameters for hillebrandite structure

	Occu- pancy	<i>x</i>	<i>y</i>	<i>z</i>	$U_{\text{eq}}$ (Å <sup>2</sup> )
Ca1	1.0	0	0.2164(2)	0.064	0.0137(5)
Ca2	1.0	½	0.3992(2)	-0.0479(3)	0.0114(5)
Ca3	1.0	½	0.0490(2)	0.1888(2)	0.0118(5)
Si1	0.5	0.430(2)	0.0863(3)	-0.1019(4)	0.011(1)
Si2	0.5	½	0.3727(5)	0.2134(6)	0.008(1)
O1	1.0	0	0.3091(6)	-0.0812(8)	0.014(3)
O2	1.0	½	0.1259(6)	0.0198(8)	0.013(3)
O3	1.0	½	0.4637(7)	0.138(1)	0.024(3)
O4	1.0	½	0.2964(7)	0.1251(9)	0.019(3)
O5	1.0	1	0.4890(6)	-0.1123(8)	0.010(3)
O6	1.0	0	0.1370(6)	0.2361(8)	0.013(3)
O7	0.5	0.364(4)	0.1328(7)	-0.205(1)	0.014(3)
O8	0.5	0	0.110(1)	-0.127(2)	0.014(3)

TABLE 3. Interatomic distances (Å) for hillebrandite

Ca1-O1	2.29(3)
O2 (× 2)	2.40(2)
O4 (× 2)	2.34(2)
O6	2.41(3)
Mean	2.36
Ca2-O1 (× 2)	2.38(2)
O3	2.43(4)
O5 (× 2)	2.46(2)
O4	2.66(4)
O6	2.62(3)
Mean	2.48
Ca3-O2	2.36(3)
O3 (× 2)	2.37(2)
O6 (× 2)	2.38(2)
O5	2.43(3)
Mean	2.38
Si1-O2	1.60(3)
O5	1.61(3)
O7	1.62(5)
O8	1.62(2)
Mean	1.61
Si2-O3	1.74(4)
O4	1.63(4)
O7 (× 2)	1.64(5)
Mean	1.66

least-squares refinement was made by refining positional parameters, anisotropic displacement factors for cations and isotropic displacement factors for anions, the scale factors, and a secondary extinction factor (a total of 59 parameters). The isotropic displacement factors for anions were employed in the final refinement because the poor diffracting quality of the crystal resulted in low observed data vs. variable ratios (~5.5). The results of the final cycle of least-squares refinement are recorded in Table 1.

The positional parameters and equivalent isotropic displacement factors are given in Table 2. Table 3 lists selected interatomic distances. Anisotropic temperature factors and observed and calculated structure factors are listed in Tables 4 and 5, respectively.<sup>1</sup>

### STRUCTURE DESCRIPTION

The hillebrandite structure consists of a three-dimensional network of Ca polyhedra connected to form tunnels parallel to [100] (Fig. 1) that accommodate isolated wollastonite-type SiO<sub>4</sub> tetrahedral chains (Fig. 2).

#### Ca-(O,OH) polyhedral network

In the asymmetric unit, there are three independent Ca positions coordinated by six (Ca1, Ca3) and seven (Ca2) anions. Each Ca-(O,OH) polyhedron shares two edges at  $x = 0$  and  $x = 0.5$  with two neighboring Ca polyhedra of the same kind to form three continuous Ca-(O,OH) polyhedral columns parallel to [100]. Ca1-(O,OH) and Ca3-(O,OH) columns share common edges to form a double chain of Ca-(O,OH) octahedral four-membered rings parallel to [100]. The Ca2-(O,OH) columns link the double

<sup>1</sup> A copy of Tables 4 and 5 may be ordered as Document AM-95-591 from the Business Office, Mineralogical Society of America, 1130 Seventeenth Street NW, Suite 330, Washington, DC 20036, U.S.A. Please remit \$5.00 in advance for the microfiche.

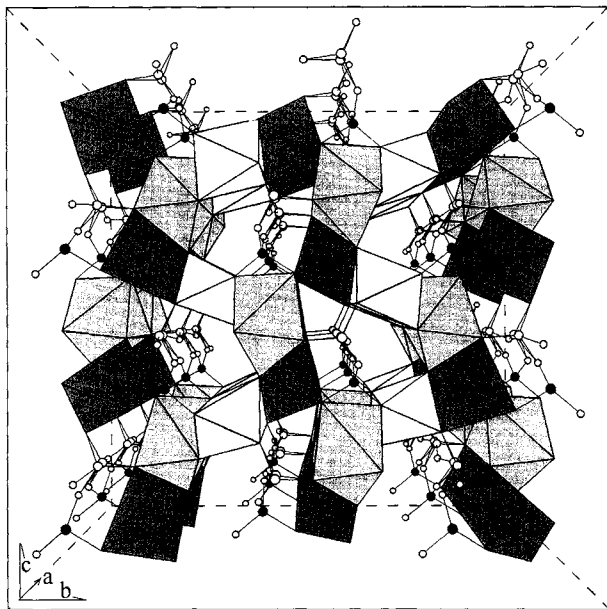


Fig. 1. Perspective view of hillebrandite structure along the *a* axis. Ca1-, Ca2-, and Ca3-(O,OH) polyhedra are shaded with light- to dark-gray colors, respectively. The Si-O tetrahedra plotted in ball-stick patterns form wollastonite-type chains accommodated in the structural channels parallel to the *a* axis (stippled circles are Si1 and black circles are Si2).

Ca1 + Ca3 chains by edge sharing to form an infinite corrugated sheet normal to *b* (Fig. 1). Between two corrugated sheets, the Ca2 polyhedra of one sheet share corners with the Ca3 octahedra of the other sheet to form a three-dimensional network of Ca-(O,OH) polyhedra. This type of arrangement of the Ca-(O,OH) columns yields structural channels between the corrugated sheets where the SiO<sub>4</sub> chains reside and reinforce the linkages between the sheets.

#### SiO<sub>4</sub> tetrahedral chain

There are two <sup>49</sup>Si sites (Si1, Si2) in the channels; each site is one-half occupied. The SiO<sub>4</sub> tetrahedra link to each other to form infinite wollastonite-type chains, the so-called dreierketten. Figure 2 shows the paired (Si1O<sub>4</sub>) and bridging (Si2O<sub>4</sub>) tetrahedra kinked so as to repeat at intervals of three tetrahedra. These wollastonite-type chains were also found in foshagite (Gard and Taylor, 1960) and tobermorite (Hamid, 1981) and have been speculated to occur in many other calcium silicate hydrate phases with a common short unit-cell translation of ~3.64 Å or 2 × 3.64 Å (Gard and Taylor, 1976; Gard et al., 1977; Taylor, 1986, 1992; Richardson and Groves, 1992; Cong and Kirkpatrick, 1993). In each structural channel (Figs. 1 and 2), there are two symmetrically equivalent dreierketten related by the mirror plane perpendicular to *a*; however, only one dreierkette can exist in a given channel to give reasonable interatomic distances; that is, in any given channel the Si and O atoms are ordered into one set of the dreierkette sites. This ordering scheme apparently

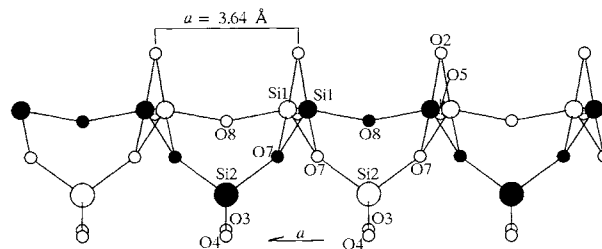


Fig. 2. The [010] projection of two equivalent Si<sub>3</sub>O<sub>8</sub> tetrahedral chains (one filled black, the other in white) in each structural channel. Si2, Si1, and O atoms are shown as large to small circles, respectively.

does not affect the distribution of the Si and O atoms in the next channel; no evidence was observed for long-range ordering of the SiO<sub>4</sub> chains in different channels, which would result in doubling of the *a* axial length as suggested by Heller (1953) and Ishida et al. (1992). Our preliminary electron diffraction investigations along *a*, *b*, and *c* axes on the specimen used in this study showed weak striations at 1/2*a* in the *a*\* and *b*\* reciprocal plane, suggesting only short-range ordering of the SiO<sub>4</sub> dreierkette chains possible in a given crystal domain. Further TEM work is warranted to understand the mechanism of short-range ordering.

#### OH groups

On the basis of Pauling's electrostatic valence rule, the results of bond-valence calculations (Table 6) were used to distinguish O atoms, OH groups, and H<sub>2</sub>O molecules in the refined structure as suggested by Donnay and Allmann (1970). Of the eight O sites, the O1 and O6 appear to be OH groups, which account for two-thirds of the H<sub>2</sub>O content in the chemical formula. In fact, there are positive electron-density anomalies near the O1 and O6 sites on the final difference map. Nevertheless, the data set available does not allow positive assignment of the H positions (Nelson and Guggenheim, 1993). The fully occupied O3 and O4 sites, however, bond to a half-occupied Si2 site (Fig. 2, Table 6). Apparently, when the Si2 site is occupied, the O3 and O4 sites achieve normal bond valences. When the Si2 site is vacant, however, the O3 and O4 sites are substantially underbonded, suggesting OH groups at the O3 and O4 sites. Thus, the O3 and O4 sites are half-occupied by O atoms (Si2 site occupied) and half-occupied by OH groups (Si2 site vacant), accounting for the remaining one-third of the H<sub>2</sub>O in the structure. The anisotropic coordination environments around O3 and O4 may explain the large displacement factors of the sites relative to other O sites (Table 2) and the abnormally long Si2-O3 (1.74 Å) bond. Nevertheless, the X-ray diffraction data do not support positional disorder for the O3 or O4 sites.

#### RELATED STRUCTURES

Numerous X-ray diffraction studies and recent NMR studies have shown that the majority of CSH phases in

TABLE 6. Bond valences (vu) for hillebrandite

Atom	O1	O2	O3	O4	O5	O6	O7	O8	$\Sigma$
Ca1	0.42	0.31 <sup>x2</sup> ↓		0.36 <sup>x2</sup> ↓		0.30			2.15
Ca2	0.33 <sup>x2</sup> ↓		0.29	0.15	0.26 <sup>x2</sup> ↓	0.17			1.79
Ca3		0.35	0.34 <sup>x2</sup> ↓		0.29	0.33 <sup>x2</sup> ↓			1.98
Si1		1.07			1.04		1.01	1.01 <sup>x2</sup> ↓	4.13
Si2			0.73	0.98			0.96 <sup>x2</sup> →		3.63
$\Sigma$	1.08	2.04	1.70	1.85	1.76	1.13	1.97	2.02	
			0.97*	0.87*					

Note: constants are from Brese and O'Keeffe (1991); the arrows indicate the bond-valence summation direction.

\* Bond-valence sums of O3 and O4 when Si2 sites are vacant.

steam-cured Portland cement have wollastonite-type dreierketten in their structures, characterized by a common translation of about 3.64 Å or  $2 \times 3.64$  Å in one cell direction (Taylor, 1986, 1992; Richardson and Groves, 1992; Cong and Kirkpatrick, 1993). Natural minerals in the CaO-SiO<sub>2</sub>-H<sub>2</sub>O system can be arbitrarily divided into two groups: one with the common short axis of about 3.64 Å or  $2 \times 3.64$  Å (hillebrandite, jennite, tobermorite, foshagite, nekoite, etc.) and the other without this feature (afwillite, reyerite, gyrolite, jaffeite, etc.). The phases in the first group, hereafter called cement minerals, are analogous or similar to the CSH phases in steam-cured Portland cements.

The Ca-Si ratios of the cement minerals vary from 2:1 (hillebrandite) to 1:2 (nekoite), which is within the range (2.5:1 to 1:2.5) of synthetic phases summarized by Taylor (1986) and Richardson and Groves (1992). Among the numerous cement minerals only five structures are known experimentally: hillebrandite (this study), tobermorite (Hamid, 1981), foshagite (Gard and Taylor, 1960), okenite (Merlino, 1983), and nekoite (Alberti and Galli, 1980). The wollastonite-type SiO<sub>4</sub> and Ca-(O,OH) polyhedral chains parallel to the short axis are the common structural units found in these minerals. The arrangements of the structural units vary with the ratios of Ca-Si. In nekoite and okenite, Ca-Si = 1:1.8 and 2.0, respectively, two wollastonite-type SiO<sub>4</sub> chains are linked together to form double chains. Some of the double chains interconnect to form SiO<sub>4</sub> tetrahedral sheets. Between these tetrahedral sheets are the remaining SiO<sub>4</sub> double chains and all Ca-(O,OH) chains. In foshagite and tobermorite, Ca-Si = 1:1 and 1:0.8, respectively; instead of SiO<sub>4</sub> tetrahedral sheets, Ca-(O,OH) polyhedral sheets sandwich the SiO<sub>4</sub> wollastonite-type chains and the remaining Ca-(O,OH) chains. In hillebrandite, with Ca-Si = 2:1, the Ca-(O,OH) polyhedral chains interconnect into a three-dimensional network in which the SiO<sub>4</sub> dreierketten chains are accommodated. Thus, there are at least three major structure types among the cement minerals with Ca-Si ratios varying from 0.5 to 2.0, represented by nekoite (0.5), tobermorite (0.8), and hillebrandite (2.0). The Ca-Si ratios that mark the transition points from one type to another are not known. Further structure investigations of other known cement minerals are essential for advancing our understanding of the structural relationships

among cement minerals as well as synthetic CSH phases with various Ca-Si ratios.

### ACKNOWLEDGMENTS

The Smithsonian Institution is acknowledged for support through a Smithsonian Postdoctoral Fellowship to Y.D. Y.D. thanks Harbison-Walker Refractories for supporting the final stage of manuscript preparation. TEM work was conducted at the Johns Hopkins University with assistance from Huifang Xu. Thorough and constructive reviews of the manuscript were provided by George E. Harlow and Carl A. Francis.

### REFERENCES CITED

- Alberti, A., and Galli, E. (1980) The structure of nekoite, Ca<sub>2</sub>Si<sub>6</sub>O<sub>15</sub>·7H<sub>2</sub>O, a new type of sheet silicate. *American Mineralogist*, 65, 1270–1276.
- Brese, N.E., and O'Keeffe, M. (1991) Bond-valence parameters for solids. *Acta Crystallographica*, B47, 192–197.
- Cong, X.D., and Kirkpatrick, R.J. (1993) <sup>17</sup>O and <sup>29</sup>Si MAS NMR study of β-C<sub>2</sub>S hydration and the structure of calcium-silicate hydrates. *Cement and Concrete Research*, 23, 1065–1077.
- Donnay, G., and Allmann, R. (1970) How to recognize O<sup>2-</sup>, OH<sup>-</sup> and H<sub>2</sub>O in crystal structures determined by X-rays. *American Mineralogist*, 55, 1003–1015.
- Fair, C.K. (1990) Molen: Structure determination system. Enraf-Nonius Delft Instruments X-ray Diffraction B.V., the Netherlands.
- Gard, J.A., and Taylor, H.F.W. (1960) The crystal structure of foshagite. *Acta Crystallographica*, 13, 785–793.
- (1976) Calcium silicate hydrate (II) ("C-S-H(II)"). *Cement and Concrete Research*, 6, 667–678.
- Gard, J.A., Taylor, H.F.W., Cliff, G., and Lorimer, G.W. (1977) A re-examination of jennite. *American Mineralogist*, 62, 365–368.
- Hamid, S.A. (1981) The crystal structure of the 11 Å natural tobermorite Ca<sub>2.25</sub>[Si<sub>4</sub>O<sub>7.5</sub>(OH)<sub>1.5</sub>]·1H<sub>2</sub>O. *Zeitschrift für Kristallographie*, 154, 189–198.
- Heller, B.A. (1953) X-ray investigation of hillebrandite. *Mineralogical Magazine*, 30, 150–154.
- Ishida, H., Mabuchi, K., Sasaki, K., and Mitsuda, T. (1992) Low-temperature synthesis of β-Ca<sub>2</sub>SiO<sub>4</sub> from hillebrandite. *Journal of the American Ceramic Society*, 75, 2427–2432.
- Merlino, S. (1983) Okenite, Ca<sub>10</sub>Si<sub>18</sub>O<sub>46</sub>·18H<sub>2</sub>O: The first example of a chain and sheet silicate. *American Mineralogist*, 68, 614–622.
- Nelson, D.O., and Guggenheim, S. (1993) Inferred limitations to the oxidation of Fe in chlorite: A high-temperature single-crystal X-ray study. *American Mineralogist*, 78, 1197–1207.
- Richardson, I.G., and Groves, G.W. (1992) Models for the composition and structure of calcium silicate hydrate (C-S-H) gel in hardened tricalcium silicate pastes. *Cement and Concrete Research*, 22, 1001–1010.
- Taylor, H.F.W. (1986) Proposed structure for calcium silicate hydrate gel. *Journal of American Ceramic Society*, 69, 464–467.
- (1992) Tobermorite, jennite and cement gel. *Zeitschrift für Kristallographie*, 202, 41–50.

MANUSCRIPT RECEIVED JUNE 23, 1994

MANUSCRIPT ACCEPTED MARCH 29, 1995